Distribution of Uronate Residues in Alginate Chains in Relation to Alginate Gelling Properties

Bjørn T. Stokke,*,† Olav Smidsrød,‡ Per Bruheim,‡ and Gudmund Skjåk-Bræk‡

Norwegian Biopolymer Laboratory, Department of Physics and Division of Biotechnology, University of Trondheim, NTH, N-7034 Trondheim, Norway

Received January 2, 1991; Revised Manuscript Received March 19, 1991

ABSTRACT: Alginate is a family of polysaccharides isolated from seaweeds or produced by certain bacteria composed of (1→4)-linked residues of α-L-guluronic acid (G) and β-D-mannuronic acid (M) varying both in abundance and sequence along the chain. Chain sequences from five different sources were reconstructed by using experimentally determined fractions of the eight possible triad arrangements as parameters in second-order Markov chains. The Monte Carlo generated chain sequences were analyzed with respect to gelling ability, assuming a cooperative model for junction formation. The cooperative model was approximated by a step function at LG_{min} representing the minimum level of G blocks being able to form a junction. By varying LG_{min} from 4 to 12, it was found that there was a fraction, the loose-end fraction, of chains within each sample that had less than two possible junction zones. The loose-end fraction was calculated to decrease with increasing chain length and with decreasing LG_{min}. The gel strength was found to correlate to the calculated number of elastically active chains. The sol fraction constitutes chains with no G blocks of length exceeding LG_{min}. The sol fraction was found to depend on the source of the alginate, to decrease with increasing chain length and decreasing LG_{min}, and to constitute approximately 35–50% of the loose-end fraction. The sol fraction was further predicted to be enriched in β-D-mannuronic acid residues, the enrichment being larger for smaller LG_{min}. The model unites properties at the polymer level to those of practical interest, such as gel strength and porosity and enrichment of β-D-mannuronic acid in leaking material, properties that are of prime importance when applying alginates as immobilization material for implantation purposes.

Introduction

Alginate is a family of polysaccharides composed of (1→4)-linked residues of β-D-mannuronic acid (M) and α-L-guluronic acid (G) in varying proportions and sequence along the chain.[1] It forms gels with most divalent cations (e.g., Ca^{2+}), and the use of calcium alginate gel beads for entrapment of living or dead cells both in vitro and in vivo is a very promising technique in biotechnology and biomedical technology.[2] The design of the optimum gel bead for a specific application requires a detailed understanding of the gelling mechanism and how the different primary structures influence properties such as gel strength and porosity, diffusional properties of molecules of varying sizes in and out of the beads, long-term stability of the beads, leakage of alginate molecules out of the beads.[2]

It is well-known that sequences containing more than one G residue combine with other similar sequences binding calcium ions in between them to form junction zones in calcium alginate gels in the so-called egg-box model.[3,4] Several reports also indicate that such cooperative ionotropic gelation only occurs when the length of the G blocks involved in the dimerization exceeds a certain length.[5,6] In this study we will first summarize the experimental evidence for the cooperative nature of alginate gelation. The formalized cooperative model is subsequently approximated with a step function for the probability of junction formation versus the number of contiguous G units in a block. The step is occurring at LG_{min}. The main emphasis in the present paper is to see how LG_{min} and the block length distribution at a specific molecular weight affect the ability to form junction zones. Block length distributions for various alginate sources will be reconstructed consistent with experimentally determined triad occurrence using NMR methods. The results of the simulations will be tested on some already reported experimental evidence and on some novel results from experiments addressing leakage of alginate polymer molecules from alginate gels.

* Address correspondence to this author.
† Department of Physics.
‡ Division of Biotechnology.

Theory

Development of a Cooperative Model for Junction Formation. The binding of calcium ions to contiguous sequences of guluronic acid has been found to be strongly cooperative both in alginate fragments enriched in guluronic acid[5] and in intact alginate.[1,7] The egg-box model for the gelation of alginate caused by divalent metal ions is the currently accepted model for the side-by-side arrangement of oligoguluronic acid sequences in the junction zones.[3,4] Less detail is known about the length of the guluronic acid blocks making up the junction zones. Gelation studies on alginates from different sources indicate a phenomenological correlation between the modulus of elasticity and the average length of those *G* blocks larger than one residue, $L_{G>1}$.[6] However, a leveling off of the gel strength when the average length of those G blocks exceeded about 10 was observed. The binding of Ca^{2+} ions to oligoguluronate of different lengths showed a marked increase at a degree of polymerization of about 10–15, after which the binding became independent of chain length.[8,9] From the temperature dependence of the evolution of the storage modulus of a gelling alginate solution it was deduced that the average length of the junction zones in the gel under formation was of the order of 20 units.[10] It appears therefore that at a given physical condition there is a minimum length of the G blocks needed for formation of a junction, although the exact length is not known unambiguously at present. No gelation was observed for alginates comprised of strictly alternating sequences, thus the minimum G-block length is at least 2.[11]

Some more information can be obtained by applying a near-neighbor autocooperative model for binding of Ca^{2+} ions in junction zones.[5] With such a cooperative model for dimerization of oligoguluronic acid residues of a finite

0024-9297/91/2224-4637$02.50/0

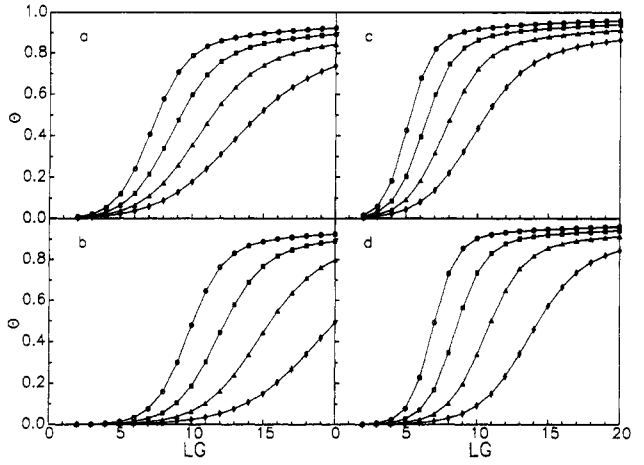

Figure 1. Calculated probability for junction formation, θ, versus degree of polymerization n (LG) at T = 10 °C (○), 30 °C (□), 50 °C (△), and 70 °C (◇) for $\sigma = 10^{-3}$ (a, c) and 10^{-4} (b, d) and ΔH = 6 (a, b) and 9 kJ mol^{-1} (c, d).

length with degree of polymerization n, the fraction of chain sequences binding calcium ions and therefore participating in a junction is given as (see, e.g., Cantor and Schimmel[12])

$$\theta(s) = \frac{\sigma s}{(s-1)^3} \frac{ns^{n+2} - (n+2)s^{n+1} + (n+2)s - n}{n(1 + [\sigma s/(s-1)^2][s^{n+1} + n - (n+1)s])} \quad (1)$$

where s is the equilibrium constant in the elongation of a junction zone with one unit and σ is the additional penalty associated with the initiation of a junction. One of the contributions to σ is from the loss of independent diffusibility of the two joining oligouronides. The parameter s plays the equivalent role of temperature and is given by a van't Hoff relation:

$$\ln s = \frac{\Delta H}{R}\left(\frac{1}{T_m} - \frac{1}{T}\right) \quad (2)$$

where ΔH is the negative of the enthalpy gain associated with elongation of the junction zone with one residue, R the molar gas constant, T_m the Kelvin temperature where an infinitely long chain has half of its residues involved in a junction, and T the actual Kelvin temperature. ΔH is here given per mole of guluronic acid residues, which is four times the binding enthalpy of the Ca^{2+} ions because each ion is coordinated to four G residues.[3,4] Only even values of n have physical significance in the description since the egg-box model specifies that two and two residues join the growing junction zone at a time. Any kinetic hindrance to the optimal utilization of G blocks in junction formation as well as further side-by-side aggregation of junction zone dimers to form microcrystallites is not considered in the present description.

Figure 1 shows calculated fraction of chain sequences involved in a junction formation versus oligoguluronic acid length at four different temperatures (eqs 1 and 2). The calculations were carried out assumming a high degree of cooperativity, $\sigma = 10^{-3}$ (a and c) and 10^{-4} (b and d), the melting temperature of alginate gels is arbitrarily set to T_m = 140 °C, and the ΔH is set to 6 (a and b) and 9 kJ/mol (c and d). The value of ΔH was selected to double that experimentally determined for binding of Ca^{2+} to guluronic acid.[13] We are not aware of any reports on experimental determination of T_m for alginate gels, nor is the degree of cooperativity explicitely reported. However, T_m is not localized below the boiling point of water, and we adopted a physically reasonable value for this parameter. Likewise, the modeling selectivity of alginate for binding of Ca^{2+} relative to Mg^{2+} [5] suggests that σ is within the values selected for the illustration. The characteristic feature of Figure 1 is that short sequences are not able to form junctions, whereas a cooperative transition to the ability to form a junction is encountered on increasing the sequence length of the G blocks. Figure 1a,b further shows that the midpoint of the transition is an increasing function of T for constant ΔH and a decreasing function of ΔH for constant T. The present description shows a clear tendency for a cooperative binding qualitatively in the same size range where the activity coefficient of Ca^{2+} showed a marked drop, between 10 and 15 residues.[9]

In the analysis of the ability of an alginate chain to form a junction, the cooperative transition is approximated by a step function at the nearest integer of G block length referred to as LG_{min}. The effect of this parameter on the calculated properties will be discussed explicitly. Although this is a rather crude approximation of a cooperative model for the formation of junctions, the model is simple in the sense that it contains only one parameter. If the full description is used, the σ parameter needs more adequate numerical estimates in the simulations than used above (Figure 1). Furthermore, it is anticipated that the results for the two-parameter model would correspond to a weighted average over the results of the one-parameter approximation. Thus the complexity will increase, the uncertainty in parameter estimation will affect the results, without adding physical insight into the problem. We therefore limit ourselves to the simple one-parameter model in the present calculations to see to what extent experimental data can be given a meaningful interpretation.

Calculations of Block Length Distributions in Alginate. The description of the primary structure of alginate is in itself a formidable task. Using NMR methods, the monad, diad, and triad frequencies can be determined[14-16] and used to test different statistical descriptions of monomer sequence in a binary chain. On the basis of the currently available experimental data, it seems that the alginate chain can best be described by second-order Markov statistics, i.e., that the probability of occurrence of a certain type of monomer residue (M or G) depends on the identity of the two preceding monomer residues. This model is also referred to as the penultimate model in the polymerization of synthetic copolymers.[17,18] However, the mechanism of the biosynthesis of alginate where poly(mannuronic acid) is epimerized at the polymer level by a C(5)-mannuron epimerase single-attack mechanism suggests that such a description is an oversimplification.[19] More recent experimental evidence suggests that multiple-attack action is a more adequate description of the epimerization at the polymer level,[20] but a full experimental characterization and a theoretical description of such an enzyme mechanism, and its consequences for the introduced monomer sequence, await further investigations. In addition, commercial samples of alginate can be produced from different types of seaweeds with differences in the chemical compositions and blended to a final average composition. In such cases, determination of triad frequencies in combination with any statistical model is insufficient to describe the monomer sequence and the compositional heterogeneity of a population of alginate chain molecules. At present, the best approach to an alginate sample with desired primary structure is to use commercial samples only when it is known that they are isolated exclusively from one algal species or to prepare the alginate in the laboratory from a certain seaweed or, in cases where we know how the composition varies in different parts of the plants,[21] to prepare the alginate from a certain algae tissue. By measuring triad frequencies

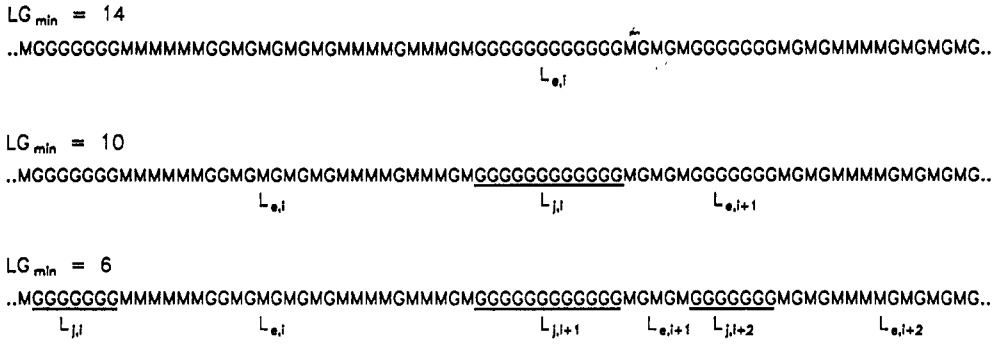

Figure 2. Identification of individual junction zones, $L_{j,i}$, and elastic units, $L_{e,i}$, within a *M. pyrifera* chain fragment when LG_{min} = 14, 10, and 6.

and applying second-order Markov statistics to the results, the present best approximation of the description to the alginate chain population may be obtained.

Fractional occurrence of trisaccharide sequences in alginate molecules provides estimates of transition frequencies in a second-order Markov model. If higher order Markov statistics are needed to give an adequate representation of alginate sequences, the extension is straightforward in the matrix formulation used to describe such chains.[22-24] When the conditional transition probabilities are specified, the relative abundance of any sequence of a given length is calculable. The first residue of a chain is determined by the fraction of G and M in the sample and put into the appropriate elements of the matrix $\mathbf{P}_0$:[22-24]

$$\mathbf{P}_0 = \begin{pmatrix} p_G & 0 & 0 & 0 \\ 0 & p_G & 0 & 0 \\ 0 & 0 & p_M & 0 \\ 0 & 0 & 0 & p_M \end{pmatrix} \tag{3}$$

where matrix element p_x is the probability of observing residue x which is equal the fraction F_x of x = G or M in the sample. The second residue is then added to first depending on whether the first residue is a M or a G as specified in the matrix $\mathbf{P}_1$:

$$\mathbf{P}_1 = \begin{pmatrix} p_{GG} & 0 & 0 & 0 \\ 0 & p_{GM} & 0 & 0 \\ 0 & 0 & p_{MG} & 0 \\ 0 & 0 & 0 & p_{MM} \end{pmatrix} \tag{4}$$

where the notation p_{xy} is used for the conditional probability of observing y when the predecessor was x and x, y = G or M. The conditional probability p_{xy} is obtained from the experimentally determined diad F_{xy} and monad F_x fractions as F_{xy}/F_x and x, y = G or M. Analogously, the third and consecutive residues are added to the chain based on the occurrence of the two preceding residues:

$$\mathbf{P}_2 = \begin{pmatrix} p_{GGG} & p_{GGM} & 0 & 0 \\ 0 & 0 & p_{GMG} & p_{GMM} \\ p_{MGG} & p_{MGM} & 0 & 0 \\ 0 & 0 & p_{MMG} & p_{MMM} \end{pmatrix} \tag{5}$$

In this matrix, p_{xyz} is used for the conditional probability of observing z when the sequence of the two previous was xy, and x, y, z = G or M. The experimentally determined triad, F_{xyz}, and diad, F_{xy}, fractions are used to calculate the conditional probabilities as $p_{xyz} = F_{xyz}/F_{xy}$. Any sequence an alginate chain with degree of polymerization DP is thus contained in the matrix product $\mathbf{P}_0\mathbf{P}_1\mathbf{P}_2^{DP-2}$. The probability of observing a specified sequence can be extracted by using the matrix elements. Likewise, averages of block length distributions are calculable on the basis of conditional probabilities. Although length distributions of homopolymeric blocks are also analytically calculable by using the conditional probabilities in the second-order Markov chain, we adopted a Monte Carlo approach because this method directly provide chemical heterogeneity within the sample, which is central to the gelation properties under investigation.

The calculations were carried out for realistic alginate samples (see below) that were well described in terms of relative abundance of triads by NMR methods. The same samples are also described as to their gelling properties[6,25] and diffusion properties of bovine serum albumin inside such gels,[26] thus providing us with experimental data allowing evaluation of the theoretical predictions. The second-order Markov model is first used to reconstruct polymer sequences based on experimentally determined NMR data. Figure 2 shows a reconstructed segment of alginate from *Macrocystis pyrifera*. The sequences of contiguous guluronic acid of length equal to or larger than the specified LG_{min} are classified as being able to form a junction, $L_{j,i}$ in Figure 2, whereas the shorter guluronic acid sequences interspersed with mannuronic acid sequences of varying length make up the elastic chains, $L_{e,i}$ in Figure 2, joining the possible junction zones. There was no discrimination between possible junction zone formation on the basis of the length of the joining elastic units, nor were very long G blocks, e.g. exceeding 40 residues, allowed to participate in more than one junction.

Chains that possess less than two G-block sequences of length equal to or larger than the specified LG_{min} will not propagate the connectivity of the polymer network and contribute to the equilibrium elasticity; e.g., the sample chain in Figure 2 considered for LG_{min} = 10 is such a chain. Those chains that have only one G block larger than LG_{min} may bind to the gel but will constitute only a loose end and are referred to as the loose-end fraction. Chains with no G blocks of length equal to or larger than LG_{min} are not able to bind to the network under the present assumption and are referred to as the sol fraction (e.g., the chain in Figure 2 considered for LG_{min} = 14). The sol fraction is able to leak out of the gel. The following properties were calculated for the alginates listed in Table I: the loose-end and sol fraction for LG_{min} ranging from 4 to 20 and degree of polymerization, DP, from 50 to 2000; the average length of junction zones L_j, average number of junction zones per chain N_j, and the average length of the chain sequences spanning the possible junction zones L_e. The average junction functionality was calculated as $\langle f \rangle = 4 - 2\langle 1/N_j \rangle$. The chemical composition, i.e., the relative amount of the possible monads, diads, and triads, was calculated for both the sol and loose-end fraction and the remaining material.

Experimental Section

Preparation of Alginates. Sodium alginate with a high content of transition frequencies was prepared from old tissue

Table I
Alginate Sources and Chemical Composition

source	F_G	F_M	F_{GG}	F_{GM}	F_{MM}	F_{GGG}	F_{GGM}	F_{GMG}	F_{GMM}	F_{MGG}	F_{MGM}	F_{MMG}	F_{MMM}	$L_{G>1}$	E, N cm^{-2}
A. nodosum	0.43	0.57	0.20	0.23	0.34	0.12	0.08	0.12	0.11	0.08	0.15	0.11	0.23	3.5	3.2
M. pyrifera	0.42	0.58	0.22	0.20	0.38	0.17	0.05	0.14	0.06	0.05	0.15	0.06	0.32	5.4	4.9
L. digitata	0.40	0.60	0.26	0.14	0.46	0.22	0.04	0.06	0.08	0.04	0.10	0.08	0.38	7.5	4.0
L. hyperborea	0.68	0.32	0.56	0.12	0.20	0.51	0.05	0.07	0.05	0.05	0.07	0.05	0.15	12.2	8.9
L. hyperborea (out. c.)	0.75	0.25	0.66	0.09	0.16	0.62	0.04	0.05	0.04	0.04	0.05	0.04	0.12	17.5	9.6

of *Ascophyllum nodosum* and an alginate rich in guluronic acid was isolated from the outer cortex of the stipes of 6–8-year-old plants of *Laminaria hyperborea*, as described by Haug.[21] A commercial sample of alginate from *Laminaria digitata* was obtained from Grinstedt, Denmark. Alginate from *L. hyperborea* stipe (LF-10/60) was obtained from Protan Biopolymers A/S Drammen, Norway. A sample prepared from *M. pyrifera* was obtained from Kelco Division of Merck, San Diego, CA. The commercial alginates were purified by dissolution in 0.2% aqueous sodium chloride, followed by precipitation with ethanol and washing with ethanol and ether before drying.[11]

NMR Spectroscopy. The proton spectra were recorded at 92 °C on a Bruker WM-500 or a Jeol FX-100 spectrometer. The latter spectrometer was also used to obtain the 25-MHz ^{13}C NMR spectra. The monomer composition and diad and G-centered triad frequencies were determined from the ^1H spectra as described previously,[14] and the M-centered triads were obtained from the ^{13}C spectra.[16] The compositional data are given in Table I.

Leaking of Alginate from Alginate Gels (Preparative). The gel beads were prepared by allowing droplets of aqueous sodium alginate (200 mL, 2% w/v) to fall into an aqueous solution of calcium chloride (0.1 M). The viscous solution was pressed through a syringe (1.0 mm) and the size of the droplets was controlled by applying a coaxial air stream.[25] The same procedure was followed for production of Sr^{2+} and Ba^{2+} beads. The gel beads were then kept in the $CaCl_2$, $SrCl_2$, or $BaCl_2$ solution for 24 h. They were 2 mm in diameter and had a final polymer content after correction for shrinkage of 2.6–3.4% w/v. The beads were washed with distilled water and suspended in 500 mL of saline (0.9% NaCl). The beads were kept at 4 °C on a gyratory shaker and the sodium chloride solution was changed every 4 days. The sodium chloride solutions were pooled, concentrated by evaporation, and dialyzed against 0.05 M EDTA, pH 7.0, for 24 h and exhaustively against water. The soluble polymeric material was collected by freeze-drying.

Leaking of Alginate (Analytical). Calcium, strontium, and barium alginate beads were formed as described above from 10 mL of 1.5% sodium alginate. After gelling had been completed the beads were suspended in 100 mL of saline. The leaking material was analyzed as the total soluble carbohydrate according to Dubois and co-workers.[27]

Results and Discussion

Prediction of Block Length Distributions. Figure 3 shows the calculated guluronic (a) and mannuronic (b) block length distributions for three of the sources included in this study. There is good agreement between the distributions of both G and M residues calculated directly from the conditional probabilities and those obtained from a Monte Carlo generated ensemble comprising 950 chains each with 700 residues. Figure 3 illustrates that the average block lengths calculable directly from NMR data (Table I) only yield averages within a wide distribution similar to a specific molecular weight average within a molecular weight distribution. The calculated block length distributions may be experimentally tested, i.e., the validity of applying the second-order Markov model to describe the sequential occurrence of G and M in alginate, by direct observations of G and M block length distributions from alginate samples either completely and specifically depolymerized in M blocks yielding the G block distribution or vice versa using specific enzymes.[28] Such tests can only be devised for calculations based on experimentally determined triad fractions and enzyme digestions carried out on the same alginate sample. This is so because there are large variations in chemical heterogeneity from source to source, seasonal variations within each source, and even a small variation within each batch prepared from a given source. The recently reported block length distributions[29] are examples of experimental evidence that may be useful in a critical evaluation of the present model; however, for the reasons stated above, the cited data are of limited value to test the present calculations since corresponding compositional information was not provided.

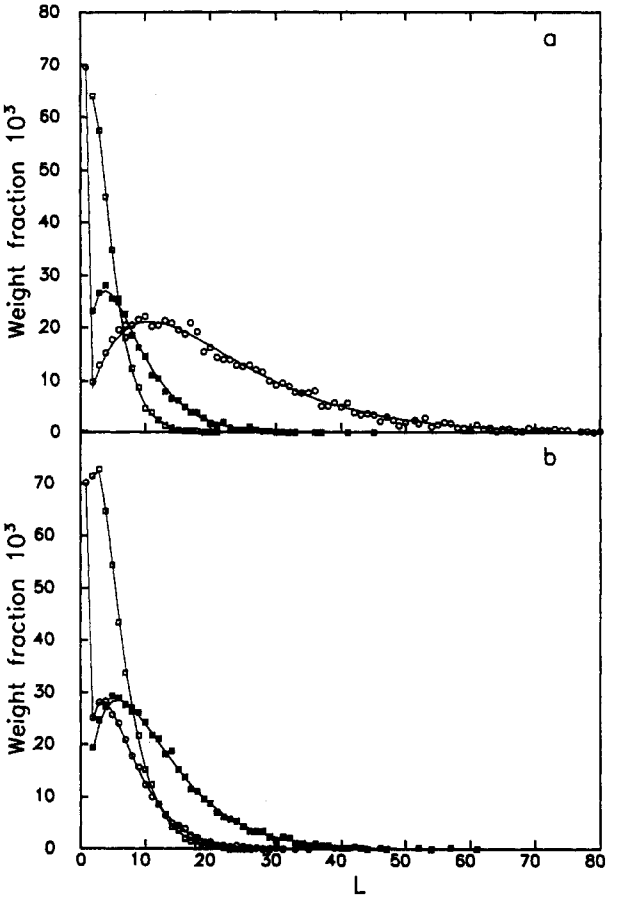

Figure 3. Weight distributions of G blocks (a) and M blocks (b) for alginate from *A. nodosum* (□), *M. pyrifera* (■), and *L. hyperborea* (○). The full drawn lines are those calculated from the conditional probabilities directly for each of the alginate sources. The Monte Carlo simulations were carried out for monodisperse samples containing totally 950 Monte Carlo generated chains with degree of polymerization 700. The weight fractions of the monads (Table I) are outside the scale for some of the sources.

Predictions of Alginate Gelling Properties. Figure 4 shows the calculated loose-end fraction versus degree of polymerization, DP, for the five alginate samples characterized (Table I) for $LG_{min} = 8$ (a) and $LG_{min} = 12$ (b). The loose-end fraction is decreasing with increasing DP for a given LG_{min} within all the samples. The increased probability of observing two or more G blocks with lengths equal to or larger than LG_{min} with increasing DP accounts for this finding. The 50% percentiles of the loose-end fraction for the *M. pyrifera* source are observed at degree of polymerization $DP_{50\%} = 159$ for $LG_{min} = 8$ increasing

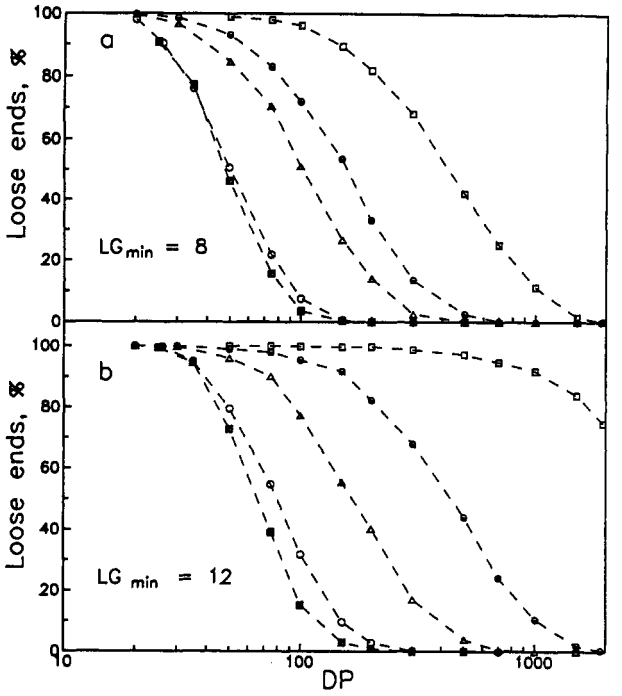

Figure 4. Loose-end fraction versus degree of polymerization for the five alginate sources from *A. nodosum* (□), *M. pyrifera* (⊖), *L. digitata* (△), *L. hyperborea* (○), and *L. hyperborea* outer cortex (⊡) The calculations were carried out for LG_{min} = 8 (a) and 12 (b).

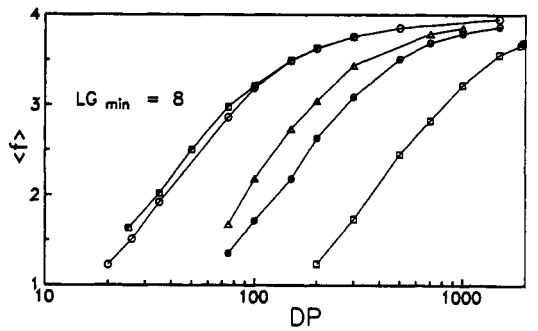

Figure 5. Average junction functionality versus degree of polymerization for the five alginate sources from *A. nodosum* (□), *M. pyrifea* (⊖), *L. digitata* (△), *L. hyperborea* (○), and *L. hyperborea* outer cortex (⊡) calculated for LG_{min} = 8.

to $DP_{50\%}$ = 440 for LG_{min} = 12, both of which are more than one order of magnitude larger than the LG_{min} values itself. Comparison of the data for the different sources reveals that, for the source *L. digitata*, 50% of the loose-end fraction is encountered at $DP_{50\%}$ = 102 at LG_{min} = 8 increasing to 167 at LG_{min} = 12. The loose-end fraction is less strongly dependent on the value of LG_{min} for this source than for the *M. pyrifera* source. This reflects that the distribution of G blocks for the *M. pyrifera* displays a stronger dependence on the block length than that for *L. digitata* around the selected values of LG_{min} (Figure 3).

Figure 5 depicts the average junction functionality $\langle f \rangle$ versus the degree of polymerization for the same five samples (Table I) for LG_{min} = 8. For all samples, we observe a change from $\langle f \rangle$ = 1 to $\langle f \rangle$ = 3.5 at a degree of polymerization depending on the source. Subsequently, there is a leveling off in $\langle f \rangle$ as the chain length increases. The source-dependent variation in the loose-end fraction and average junction functionality suggests that the lower molecular weight, M_w, needed for gels to be formed depends on the source or, likewise, that the lowest M_w above which the gel strength is independent of M_w is predicted to depend on the source of the alginate. We will here use the number-average length of G blocks larger than one unit,

Table II
Alginate Sources and Limits in DP for Gelation

	$L_{G>1}$	E, N cm^{-2}	$DP_{\langle f \rangle \to 4}$[a] at LG_{min} = 8	$DP_{\langle f \rangle \to 4}$[a] at LG_{min} = 12	$DP_{\langle f \rangle = 2}$[b] at LG_{min} = 8	$DP_{\langle f \rangle = 2}$[b] at LG_{min} = 12
A. nodosum	3.5	3.2	1780	nd	365	~3000
M. pyrifera	5.4	4.9	610	1920	126	370
L. digitata	7.5	4.0	390	910	90	185
L. hyperborea	12.2	8.9	188	291	37	63
L. hyperborea (out. cortex)	17.5	9.6	172	242	34	49

[a] $DP_{\langle f \rangle \to 4}$ denotes the degree of polymerization where the extrapolation of $\langle f \rangle$ versus DP for $1 < \langle f \rangle < 3.5$ intersects $\langle f \rangle = 4$. [b] $DP_{\langle f \rangle = 2}$ denotes the degree of polymerization where $\langle f \rangle = 2$.

$L_{G>1}$, as an index of the source because this quantity is directly calculable from the relative occurrence of triads as determined by NMR (Table I). We use $DP_{\langle f \rangle = 2}$ to denote the degree of polymerization where $\langle f \rangle$ equals 2.0. This limit represents the lowest functionality needed for a continuous network. The DP of the extrapolation of $\langle f \rangle$ equal to 4 based on $\langle f \rangle$(DP) less than 3.5 is analoguously denoted $DP_{\langle f \rangle \to 4}$. Figure 5 indicates only smaller changes in $\langle f \rangle$ above $DP_{\langle f \rangle \to 4}$; thus this parameter is indicative of a limiting molecular weight above which the gel modulus is nearly independent of molecular weight. Table II indicates that there is a correlation between $L_{G>1}$ and $DP_{\langle f \rangle = 2}$. The higher the $L_{G>1}$, i.e., the more "blocklike" the alginate type is, the lower the molecular weight needed for a gel to be formed. On an intuitive basis, the case of a strictly alternating (GM repeating copolymer) will possess no sequences of G blocks exceeding LG_{min}, independent on how large the polymer is. Thus for $L_{G>1}$ = 0, both $DP_{\langle f \rangle = 2}$ and $DP_{\langle f \rangle \to 4}$ diverge to infinity, thus giving a physical interpretation for vanishing $L_{G>1}$.

Table II presents intriguing predictions, and the experimental data to test all aspects of these characteristic molecular weights are lacking at present. The only experimental data on the molecular weight dependence of the gel strength carried out with sufficient resolution in molecular weight for the present discussion are those by Smidsrød and Haug.[30] They reported on the modulus of elasticity, E, versus DP of alginate from *L. digitata* degraded into different fractions with degrees of polymerization from 70 to 5100. The measurements were carried out on gel cylinders made by dialyzing Ca^{2+} ions into the alginate solution embodied in plastic cylinders capped with a dialysis membrane. They reported that the lower weight-average degree of polymerization, DP_w, needed in this type of alginate to form a gel was 65 and that above DP_w = 400 the modulus of elasticity was independent of DP_w. All measurements were carried out at constant polymer concentration (c = 3%), which means that the concentration relative to the overlap concentration c^* is an increasing function of DP. The reported values for onset and constancy of E are in the same size range as those predicted here for a different preparation of *L. digitata* for LG_{min} in the range 8–12 (Table II). Considering that the DPs used in the experimental study are weight averages of a polydisperse sample and that it more recently has been shown that the employed preparation procedure of the gels yields slightly nonhomogeneous gels (reflecting a kinetically trapped situation where only a fraction of the G blocks have its optimal partner in formation of junctions[31]), this agreement suggests that LG_{min} is about 8 for calcium alginate gels at 20 °C. This apparent agreement should encourage more detailed experimental investigations, including alginate of various chemical compositions in combination with various gel-inducing ions to test the model.

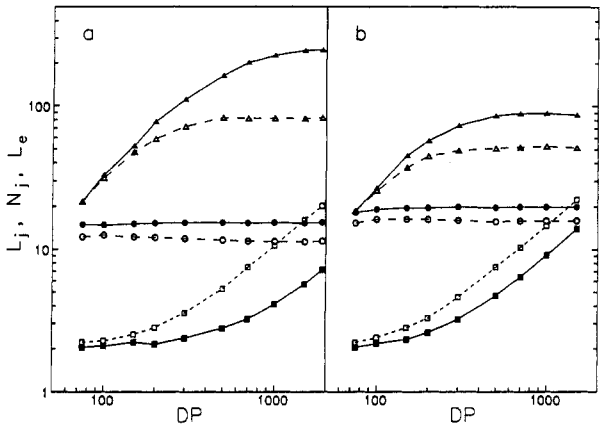

Figure 6. Chain parameters L_e (△, ▲), L_j (○, ●), and N_j (□, ■) versus degree of polymerization for alginate from *M. pyrifera* (a) and *L. digitata* (b). Calculations were carried out for LG_{min} = 8 (open symbols) and 12 (filled symbols).

Predictions of Alginate Gel Ultrastructure. We now turn to describe average properties of the alginate chains. Figure 6 shows the average values, L_j, L_e, and N_j versus the degree of polymerization for alginate from *M. pyrifera* (a) and *L. digitata* (b). These properties were calculated for the chains participating in the network; i.e., the loose-end fraction was discarded prior to evaluation. Similar calculations on the total sample including the loose-end fraction revealed chains with N_j less than 2 and even 1; see, e.g., the *M. pyrifera* segment considered under the conditions LG_{min} = 6 and 10 (Figure 2). This does not reflect the structure of the chains participating in the gel. L_j was found to be independent of DP also when a large loose-end fraction was observed (compare Figures 6a and 4a and Figures 6b and 4b), although the actual length depends strongly on the source and on the LG_{min} parameter (Table III). The parameters L_e and N_j are increasing functions of DP in the range $DP_{50\%}$ to $DP_{10\%}$ ($DP_{10\%}$ denotes 10% in the loose-end fraction of the material), whereas L_e levels off for DP larger than $DP_{10\%}$ (Figure 6). This implies that networks formed of polymer samples with DP where there is a significant loose-end fraction have smaller L_e than a network made of chains with a vanishing loose-end fraction. Even though the pore size in a gel is not directly calculable from L_e, the present calculations suggest that the pore size is smaller for an alginate with molecular weight below the critical molecular weight, giving a M_w-independent modulus of elasticity, than above.

Table III lists the calculated limiting values of L_j and L_e for DP > $DP_{10\%}$ with LG_{min} as a parameter for the given samples. L_j increases parallel with the increase in the LG_{min} for all the sources, however, the differences between L_j and LG_{min} are larger for the longer $L_{G>1}$. More profound differences are revealed in L_e: Table III reveals that L_e increases with increasing LG_{min}, though the dependence is generally stronger than for L_j except for the last entry in Table III. The reason for the increasing L_e with increasing LG_{min} is that successive G blocks of length up to LG_{min} ae excluded from the possible junction zones and included in the elastic part of the chain, thus increasing this part. How strong the actual dependence of L_e is on LG_{min} is governed by the relative abundance of G blocks at the specified LG_{min}, which again reflects the G-block distribution of the alginate chains (Figure 3). Table III also indicates that L_e is inversely related to $L_{G>1}$. The predictions thus indicate that gels of alginate with low $L_{G>1}$ should have fairly short junction zones compared to the elastic units. The length of the junctions are calculated to increase and the length of the elastic units to decrease as $L_{G>1}$ becomes longer. For the sample with the largest $L_{G>1}$, the length of the junction zones even exceeds the length of the elastic units (Table III).

The experimental evidence addressing the predictions in Figure 6 and Table III are both direct observations on the structure itself, i.e., the using electron microscopic visualization methods, and indirect probes that depend on the supramolecular structure, i.e., elasticity of the gels and diffusion of probes that are sensitive to the pore size of the polymer network. Recently, electron micrographs of gel beads made by dripping alginate solution into Ca^{2+} containing solutions for three different alginate sources were reported (Figures 4.5, 4.6, and 4.7 reported by Martinsen[26]). Although this preparation procedure might kinetically trap the gel beads in some nonoptimal condition as discussed above for gel cylinders, there is qualitative evidence in such micrographs that parallels the present theoretical predictions: For *L. hyperborea* the ultrastructure can be described as thick, rather long segments interspersed with more flexible structures that are slightly thinner. For comparison, for the alginate bead made from the *M. pyrifera* source, it appears that the rather thick filaments are reduced in length and abundance, whereas the thinner ones are more dominating.[26] However, no quantitative measurements were carried out on the micrographs. In addition, the diffusion coefficients of bovine serum albumin through alginate gels made of these two sources likewise indicate that the pore size is increasing with $L_{G>1}$.[26] Those findings are not at variance with the predictions (Table III).

Experimentally determined elasticity of alginate gels made from one type of alginate in combination with different ions was reported to correlate to the affinity between the gel-inducing ion and the polymer molecule.[1,32] This was interpreted as part of the deformation free energy was used to disrupt the junction zones of the gel.[1,32] The present model allows us to test the alternative suggestion,[33] that increasing affinity between the ion and the polymer yields increased cross-link density and not necessarily stronger junctions. Increasing the enthalpy gain associated with binding the ion to the polymer chain is predicted to reduce LG_{min} (Figure 1a,b). Thus ions that bind more strongly to the G blocks are associated with a smaller LG_{min}. LG_{min} may therefore be considered to be inversely related to the affinity of the gel-inducing ion. Reducing LG_{min}, when analyzing a particular chemical composition of alginate, is predicted both to increase the number of elastically active chains and to reduce the length of chains spanning the junction zones. These two effects increase the elastic modulus because of the increased number of elastically active chains and the increasing deviation from rubberlike elasticity. The experimental correlation between the affinity of a gel-inducing ion to an alginate chain and the gel strength may thus be related to a varying number of elastically active chains for different divalent ions.

Similarly, experimentally determined E values for gels made from different alginate types in combination with Ca^{2+} allow us to test whether the observed differences also in this case can be rationalized in terms of cross-link density. Figure 7 shows the experimentally determined[6] E versus the calculated number of elastically active chains in the corresponding alginate. The degree of polymerization was DP = 1000. This graph indicates that E is proportional to the number of elastically active chains in the gel, the scaling coefficient on this log–log plot being observed to be 0.87 for LG_{min}=6. It is expected that E depends on the number of elastically active chains irrespective of whether the free energy of deformation is mainly of entropic or enthalpic origin. The additional

Table III
Alginate Sources and Calculated Chain Characteristics

	$L_{G>1}$	L_j at LG_{min} = 6	8	10	12	L_e at LG_{min} = 6	8	10	12
A. nodosum	3.5	7.6	9.7	11.6	13.6	87.4	253	590	808
M. pyrifera	5.4	9.4	11.4	13.4	15.5	46.8	83	145	249
L. digitata	7.5	11.5	13.5	15.4	17.4	37.1	54.5	79.6	115
L. hyperborea	12.2	16.1	18.1	20.2	22.2	12.8	16.9	22.3	29.2
L. hyperborea (out. c.)	17.5	20.6	22.7	24.7	26.7	10.3	12.8	15.8	19.5

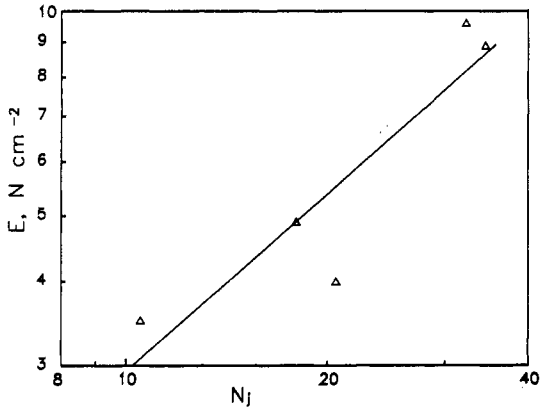

Figure 7. Modulus of elasticity versus calculated number of elastically active subchains for LG_{min} = 6. The number of elastically active chains was calculated for constant DP = 1000 for all the sources.

finding that $L_e > L_j$ in most of the cases (Table III) also indicates that disruption of junction zones during gel deformation is not likely for small strains. Concomitant with the increased number of junction zones (variation from source to source), we observed an increased L_j and a decreasing L_e (Table III). The decreased L_e indicates that departure from ideal random-coil-like behavior is more severe with a larger number of cross-links. Added to this is the fact that Table III only reports average lengths of elastic units, whereas the distribution of $L_{e,i}$ (Figure 2) contains species deviating significantly from the average. The present model therefore indicates that the experimental empirical correlation between E and $L_{G>1}$ (Figure 7 reported by Skjåk-Bræk and co-workers[6]) is due to the increasing number of elastically active chains at higher $L_{G>1}$. The present conclusion should be regarded as tentative because the number of elastically effective chains in an alginate gel depends on several factors in addition to the possibility of junction formation in each chain such as total concentration of polymer relative to the overlap concentration c^* and the procedure used to introduce the gel-inducing ion.

The calculated properties (Table III) also suggest that the complete stress–strain relationship, including the brittleness of the gels, depends on the chemical composition of the alginate chains. The gel is expected to break at a lower extension ratio for smaller L_e. This is so because Gaussian statistics for the distribution of the end-to-end distances of alginate chains is not expected for chains shorter than about 500 residues.[34] Deviations from Gaussian statistics are therefore more severe for shorter L_e, and the extensibility of the gel network before failure is thus predicted to be less for shorter L_e. Experimentally determined stress–strain relationships for alginate gels embedded in aqueous sucrose are reported to depart from that expected for rubberlike materials at strains as low as 0.13.[35] Although the alginate used was not so well characterized and also sucrose was contained in the gel, the reported[35] non-Gaussian nature is not unexpected in view of the present calculations (Table III).

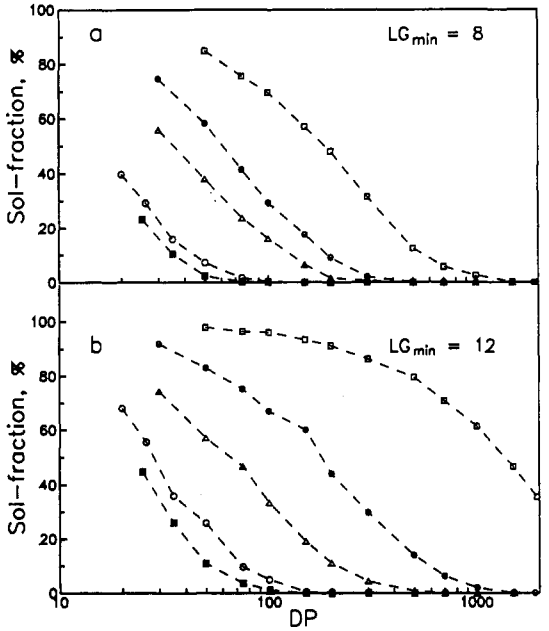

Figure 8. Sol fraction versus degree of polymerization for the five alginate sources from *A. nodosum* (□), *M. pyrifera* (●), *L. digitata* (△), *L. hyperborea* (□), and *L. hyperborea* outer cortex (▨). The calculations were carried out for LG_{min} = 8 (a) and 12 (b).

The temperature dependence of the elasticity of the polymer network provides an experimental test of the entropic or enthalpic dominance of the deformation free energy. Such an approach is also reported in the case of alginate.[35,36] Before this classical issue can be addressed, the effect of temperature on LG_{min} has to be considered. Increasing T toward T_m is predicted to increase LG_{min} (Figure 1). Increasing LG_{min} is calculated to decrease the cross-link density for a given chemical composition (Figure 6). It is thus possible, at least partly, to attribute experimentally determined decreasing $\Delta E/\Delta T$[36] to decreased cross-link density. The calculations further indicate that the temperature-dependent cross-link density varies both with the chemical composition of the alginate and the type of cross-linking ion (Figure 1). These factors should be taken into account before the nature of the deformation free energy can be assessed.

Leakage of Alginate Chains from Alginate Gels. Gels made of alginate with a DP in the range between $DP_{50\%}$ and $DP_{10\%}$ contain a fraction of chains that does not participate in the network, the sol fraction. Figure 8 shows the predicted sol fraction of alginate gels made from the sources listed in Table I versus DP calculated for LG_{min} equal to 8 (a) and 12 (b). By comparison with the loose-end fraction (Figure 4), we find that the sol fraction constitutes about half of the loose-end fraction. The source-to-source variation and the dependence on LG_{min} parallel that described for the loose-end fraction (Figure 4).

The sol fraction can be entrapped during the gelation step and later leak out from the alginate gel through a reptation process, and from an applied, biomedical point

Table IV
Alginate Sources and Calculated Chemical Composition of Sol Fraction

	original material				sol fraction					
					LG_{min} = 4		LG_{min} = 8		LG_{min} = 10	
source	F_G	F_M	F_{GG}	F_{MM}	F_M	F_{MM}	F_M	F_{MM}	F_M	F_{MM}
A. nodosum	0.43	0.57	0.20	0.34	0.60	0.36	0.57	0.34	0.57	0.34
M. pyrifera	0.42	0.58	0.22	0.38	0.70	0.48	0.63	0.42	0.61	0.40
L. digitata	0.40	0.60	0.26	0.46	0.78	0.62	0.71	0.55	0.67	0.52
L. hyperborea	0.68	0.32	0.56	0.20	0.68	0.49	0.54	0.36	0.51	0.34
L. hyperborea (out. c.)	0.75	0.25	0.66	0.16	0.47	0.34	0.48	0.33	0.46	0.31

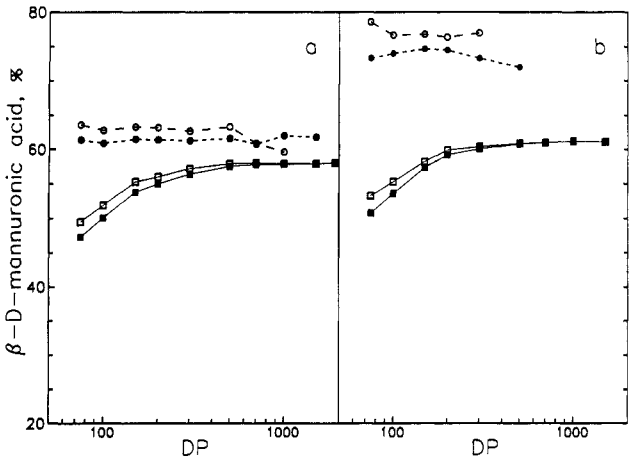

Figure 9. Calculated average content of mannuronic acid in the sol fraction (○, ●) and chains not in the sol fraction (□, ■) versus degree of polymerization for alginate from *M. pyrifera* (a) and *L. digitata* (b). The calculations were carried out for LG_{min} = 6 (open symbols) and 10 (filled symbols).

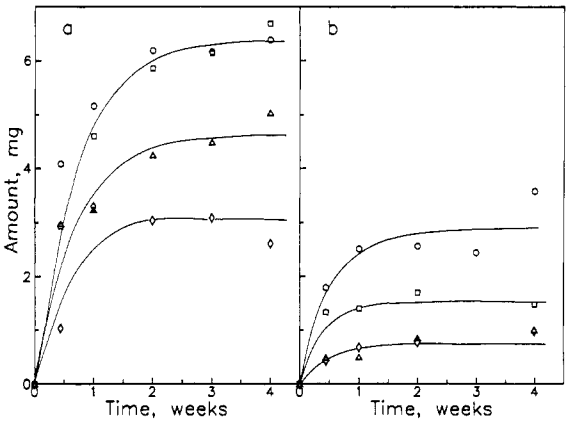

Figure 10. Amount of alginate leaked out of alginate beads versus time for alginate leakage from *M. pyrifea* (a) and *L. hyperborea* (b). Leakage data were obtained from alginate gelled and equilibrated in $CaCl_2$ (○), $BaCl_2$ (□), $SrCl_2$ (△), and $CaCl_2$ + $BaCl_2$ (◇).

of view where alginate is foreseen as immobilization material for artificial organ transplantation, it is important to be aware of such leakage. Both the amount and composition of such material are important from an immunological point of view. Figure 9 shows the predicted average content of mannuronic acid in the sol fraction and the nonsol fraction versus DP for alginate from *M. pyrifera* (a) and *L. digitata* (b) for two values of LG_{min}. The data indicate that the more blocklike alginate type produces a larger enrichment of mannuronic acid in the sol fraction (compare parts a and b of Figure 9, Table IV). The reason for this is that the composition distribution is getting broader, the shorter the alginate chain and the more blocklike the polymer is.[37]

To test the predictions presented above, we carried out experiments for measuring both the amount and the chemical composition of the material that leaked out from alginate gel beads. Figure 10 shows the amount of alginate leaking out from a total of 150 mg of alginate in gel beads made from the two alginate sources, *M. pyrifera* (a) and *L. hyperborea* (b), respectively. The accumulated amount leaking out from the beads reaches equilibrium within 2 weeks, indicating that a slow reptation process is governing the kinetics. There are differences between the two sources for a given ion type, with *M. pyrifera* alginate containing the largest amount of diffusible species. This agrees qualitatively with the prediction (Figure 8), although a quantitative correlation is not possible because the molecular weight distribution of the starting material is not known. An additional finding is that there are differences within each source depending on the type of ion used. The type of ions that is reported to have the largest affinity toward the alginate chain[32] is found to produce gels with a smaller fraction of diffusible chains (Figure 10). Similar to the intepretation given above, that increasing affinity translates to a reduction in LG_{min} thus increasing the number of elastically active chains, we find

Table V
Alginate Sources and Measured Chemical Composition of the Sol Fraction from Calcium Alginate Gel Beads

source	F_G	F_M	F_{GG}	F_{MM}	F_{MG}
A. nodosum	0.25	0.75	0.172	0.672	0.078
M. pyrifera	0.268	0.732	0.131	0.595	0.137
L. hyperborea (out. c.)	0.373	0.627	0.323	0.577	0.050

here that the experimental data corroborate semiquantitatively with the theoretical predictions, using the same interpretation of ion effects. Reduced LG_{min} as induced by, i.e., exchanging Ca^{2+} for Ba^{2+}, is predicted to reduce the sol fraction within each sample for a given DP within $DP_{10\%}$ and $DP_{50\%}$ (Figure 8). It is also recognized that these leakage studies are carried out at 4 °C, whereas increasing temperature is predicted to increase LG_{min} (Figure 1), thus influencing both the amount (Figure 8) and chemical composition (Figure 9) of the material that will leak out from the gels.

The experimentally determined monad and diad fractions of the alginate material leaking out of calcium alginate gel beads (Table V) show that the sol fraction is enriched in β-D-mannuronic acid residues. The reduction in G content within each alginate type is between 35% and 50% for the three sources studied, whereas the observed relative enrichment of M in the sol fraction ranged from 32% (*A. nodosum*) to 150% (*L. hyperborea* outer cortex). A similar effect is observed for the diad frequencies, and the relative enrichment of MM diads within each alginate type is even larger than observed for M monads. Table V shows that, for the starting material selected to have a relatively low content of mannuronic acid, the broad composition distribution of the low molecular weight tail gives diffusible species that are enriched in mannuronic acid. The more blocklike alginates are more enriched in mannuronic acid, which is in agreement with the calculations (Figure 9). Although there are rather large discrepancies between the quantitative predictions and the experiments, in particular for the sources *A. nodosum* and

M. pyrifera, there appears to be better agreement for $LG_{min} = 4$ than for higher LG_{min} for these studies carried out at 4 °C (Tables IV and V). An unknown fraction of functional chains may exist in the sol fraction due to the nonequilibrium gelation conditions used in the experiments. This could affect the quantitative correlation between the experiments and the calculations, but at present, it would represent introduction of an additional unknown variable and is therefore not considered.

It is important to be aware of such leakage because the polymannuronic blocks are the most immunostimulating parts of alginate as found in an in vitro model of monocytes.[38] Low molecular weight, highly enriched in mannuronic acid gel defective chains can be a part of a polydisperse alginate sample even if the sample has a rather large weight-average molecular weight and a fairly high average guluronic acid content. It is therefore important to control the amount of low molecular weight material in alginate samples used for immobilization of cells for subsequent implantation.

Conclusions

The present study was undertaken to add molecular understanding and quantitative predictions to a range of physical and applied biomedical properties of alginate gels. The complete alginate sequence was reconstructed, based on experimentally determined fractions of triads, diads, and monads using NMR methods assuming second-order Markov statistics. By application of a one-parameter approximation of a cooperative description for the length of G blocks involved in junction formation, properties related to gel ultrastructure, gel elasticity, and leaking of alginate material were calculated. The predictions were correlated to experiments reported by others, as well as experiments reported here. A semiquantitative agreement between the model calculations and experiments was found for alginate of different chemical compositions and for a given chemical composition in combination with different ions that have different affinities to the alginate chains.

All the predictions were based on idealized monodisperse fractions, whereas most experimental conditions are not able to meet this condition. The experiments should therefore be compared to the predicted properties averaged over the molecular weight distribution of the experimental sample. Because of such limitations in the testing of the model, we find it premature to use the agreement between the model and the experiments to establish values for LG_{min} at different physical conditions. The observed enrichment of mannuronic acid in the sol fraction is a consequence of the chemical heterogeneity of the alginate sample. The leakage studies from calcium alginate gels may indicate that the length of the cooperative unit is about 4 at 4 °C for calcium alginate gel beads, but more experiments using better characterized samples in terms of molecular weight/molecular weight distribution would be helpful in further testing of the model predictions. Such aspects are currently under investigation.

The present study unites properties at the polymer level with those of practical interest when using alginates as immobilization material. This is so for properties such as gel strength and enrichment of immunomodulating alginates in the sol fraction and possibly also for diffusional properties. In this respect, the model may provide useful guidelines for selection of alginates for various applications. The influence of the sequential arrangement of guluronic and mannuronic acid residues on the relative chain extension has been previously reported,[39] whereas the present work is the first attempt to correlate the sequence statistics to the ionotropic gelation properties.

Acknowledgment. We gratefully thank one of the reviewers for suggesting that critical molecular weights for gelation should be based on average junction functionality rather than on percentiles of the loose-end fraction. This work was partly supported by Grant BT. 1623484 from the Royal Norwegian Council for Industrial and Scientific Research and from Protan Biopolymers A/S.

References and Notes

(1) Smidsrød, O. *Faraday Discuss. Chem. Soc.* **1974**, *57*, 263.
(2) Smidsrød, O.; Skjåk-Bræk, G. *Trends Biotechnol.* **1990**, *8*, 71.
(3) Grant, G. T.; Morris, E. R.; Rees, D. A.; Smith, P. J. C.; Thom, D. *FEBS Lett.* **1973**, *32*, 195.
(4) Rees, D. A. *Pure Appl. Chem.* **1981**, *53*, 1.
(5) Smidsrød, O.; Haug, A. *Acta Chem. Scand.* **1972**, *26*, 2063.
(6) Skjåk-Bræk, G.; Smidsrød, O.; Larsen, B. *Int. J. Biol. Macromol.* **1986**, *8*, 330.
(7) Andresen, I.-L.; Skipnes, O.; Smidsrød, O.; Østgaard, K.; Hemmer, P. C. *ACS Symp. Ser.* **1977**, *48*, 361.
(8) Kohn, R.; Furda, I.; Haug, A.; Smidsrød, O. *Acta Chem. Scand.* **1968**, *22*, 3098.
(9) Kohn, R. *Pure Appl. Chem.* **1975**, *42*, 371.
(10) Lapasin, R.; Paoletti, S.; Zanetti, F. *Progress Trends Rheol.* **1988**, *II*, 422.
(11) Skjåk-Bræk, G. Dr. techn thesis, University of Trondheim NTH, Norway, 1988.
(12) Cantor, C. R.; Schimmel, P. R. *Biophysical Chemistry*; W. H. Freeman; San Francisco, 1980; III, The behavior of biological macromolecules.
(13) Cesaro, A.; Delben, F.; Paoletti, S. In *Thermal analysis*; Miller, B., Ed.; John Wiley & Sons: Chichester, 1982; Vol. II, 815.
(14) Grasdalen, H. *Carbohydr. Res.* **1983**, *118*, 255.
(15) Grasdalen, H.; Larsen, B.; Smidsrød, O. *Carbohydr. Res.* **1979**, *68*, 21.
(16) Grasdalen, H.; Larsen, B.; Smidsrød, O. *Carbohydr. Res.* **1981**, *89*, 179.
(17) Larsen, B.; Painter, T.; Haug, A.; Smidsrød, O. *Acta Chem. Scand.* **1969**, *23*, 355.
(18) Larsen, B.; Smidsrød, O.; Painter, T. J.; Haug, A. *Acta Chem. Scand.* **1970**, *23*, 726.
(19) Larsen, B. *Proc. Xth Int. Seaweed Symp.* **1981**, 7.
(20) Larsen, B.; Skjåk-Bræk, G.; Painter, T. *Carbohydr. Res.* **1986**, *146*, 342.
(21) Haug, A. Report no. 30; Norwegian Institute of Seaweed Research, 1964.
(22) Myhre, J. M. In *Markov chains and Monte Carlo calculations in polymer science*; Lowry, G. G., Ed.; Marcel Dekker Inc.: New York, 1970; p 13.
(23) Price, F. P. In *Markov chains and Monte Carlo calculations in polymer science*; Lowry, G. G., Ed.; Marcel Dekker Inc.: New York, 1970; p 187.
(24) Peller, L. *J. Chem. Phys.* **1963**, *36*, 2976.
(25) Martinsen, A.; Skjåk-Bræk, G.; Smidsrød, O. *Biotechnol. Bioeng.* **1989**, *33*, 79.
(26) Martinsen, A. Dr. Ing. thesis, University of Trondheim, NTH, Norway, 1990.
(27) Dubois, M.; Gilles, K. A.; Hamilton, J. K.; Rebers, P. A.; Smith, F. *Anal. Chem.* **1956**, *28*, 350.
(28) Haugen, F.; Kortner, F.; Larsen, B. *Carbohydr. Res.* **1990**, *198*, 101.
(29) Heyraud, A.; Leonard, C. *Food Hydrocolloids* **1990**, *4*, 59.
(30) Smidsrød, O.; Haug, A. *Acta Chem. Scand.* **1972**, *26*, 79.
(31) Skjåk-Bræk, G.; Grasdalen, H.; Smidsrød, O. *Carbohydr. Polym.* **1989**, *10*, 31.
(32) Smidsrød, O. Report no. 34; Norwegian Institute of Seaweed Research, 1973.
(33) Mitchell, J. R. *J. Texture Stud.* **1976**, *7*, 313.
(34) Bailey, E.; Mitchell, J. R.; Blanshard, J. M. V. *Colloid Polym. Sci.* **1977**, *255*, 856.
(35) Segeren, A. J. M.; Boskamp, J. V.; van den Tempel, M. *Faraday Discuss. Chem. Soc.* **1974**, *57*, 255.
(36) Andresen, I.-L.; Smidsrød, O. *Carbohydr. Res.* **1977**, *58*, 271.
(37) Smidsrød, O.; Whittington, S. G. *Macromolecules* **1969**, *2*, 42.
(38) Otterlei, M.; Østgaar, K.; Skjåk-Bræk, G.; Smidsrød, O.; Espevik, T. *J. Immunther.*, in press.
(39) Hallman, G. M.; Whittington, S. G. *Macromolecules* **1973**, *6*, 386.

Registry No. Sodium alginate, 9005-38-3